



## OPEN ACCESS

## EDITED BY

Ce Wang,  
Sun Yat-sen University, China

## REVIEWED BY

Entao Liu,  
China University of Geosciences Wuhan,  
China  
Chao Li,  
Chinese Academy of Sciences (CAS), China

## \*CORRESPONDENCE

Congjun Feng

✉ fengcj@nwu.edu.cn

Guozhang Fan

✉ fangz\_hz@petrochina.com.cn

RECEIVED 16 May 2024

ACCEPTED 02 August 2024

PUBLISHED 03 September 2024

## CITATION

Feng C, Fan G, Yang Z, Yao X, Song X, Li W, Qu H, Zhang Q and Wang X (2024) Source-to-sink processes and genetic mechanism of progradational and lateral accretion submarine fans in the Qiongdongnan Basin, South China Sea. *Front. Mar. Sci.* 11:1433826. doi: 10.3389/fmars.2024.1433826

## COPYRIGHT

© 2024 Feng, Fan, Yang, Yao, Song, Li, Qu, Zhang and Wang. This is an open-access article distributed under the terms of the [Creative Commons Attribution License \(CC BY\)](https://creativecommons.org/licenses/by/4.0/). The use, distribution or reproduction in other forums is permitted, provided the original author(s) and the copyright owner(s) are credited and that the original publication in this journal is cited, in accordance with accepted academic practice. No use, distribution or reproduction is permitted which does not comply with these terms.

# Source-to-sink processes and genetic mechanism of progradational and lateral accretion submarine fans in the Qiongdongnan Basin, South China Sea

Congjun Feng<sup>1,2\*</sup>, Guozhang Fan<sup>3\*</sup>, Zhili Yang<sup>3</sup>, Xingzong Yao<sup>1,2</sup>, Xinglei Song<sup>1,2</sup>, Weiqliang Li<sup>3</sup>, Hongjun Qu<sup>1,2</sup>, Qiang Zhang<sup>3</sup> and Xuefeng Wang<sup>3</sup>

<sup>1</sup>State Key Laboratory of Continental Dynamics, Northwest University, Xi'an, China, <sup>2</sup>Department of Geology, Northwest University, Xi'an, China, <sup>3</sup>Hangzhou Research Institute of Petroleum Geology, PetroChina, Hangzhou, China

Submarine fan reservoirs are important accumulation zones for oil, gas, and natural gas hydrates, offering significant potential for hydrocarbon exploration. During the deposition period of the Sanya Formation in the southern part of the Changchang Sag of the Qiongdongnan Basin, a large submarine fan developed. However, the internal structure, source-sink system, and formation mechanism of this fan remain poorly understood, posing significant challenges to exploration in this area. This paper examines the source-to-sink sedimentary processes and deposition of submarine fans, using the Changchang Sag, in the Qiongdongnan Basin in the Northern South China Sea, as an example, which will provide valuable general guidance for deep water oil and gas exploration. Based on the theories of seismic stratigraphy and seismic sedimentology, this paper utilizes techniques such as seismic facies analysis, seismic attribute optimization, paleogeomorphology reconstruction, and source-to-sink sedimentary system analysis to analyze the 3D seismic data of the study area. Research indicates that the Sanya Formation in the Changchang Sag of the Qiongdongnan Basin comprises three depositional units: submarine fan, feeder channel, and Semi-deep marine to deep marine mudstone. The submarine fan is a fan formed by the coupling and convergence of submarine fans sourced from the southwest and southeast. Internally, it is divided into three sub-facies: the proximal fan of the sand-rich submarine fan, the main body of the sand-rich submarine fan lobes, and the distal lobes of the sand-rich submarine fan. The submarine fan sourced from the southwest extends nearly north-south and is primarily fed by sediment transported through three large, banded ancient valleys. The sedimentary filling is characterized by three-phase progradation. The submarine fan sourced from the southeast extends nearly east-west and is

primarily fed by sediment transported through a single large, banded ancient valley. The sedimentary filling is characterized by two-phase lateral accumulation. During the deposition period of the Sanya Formation, certain areas of the southern uplift belt were exposed for extended periods and subjected to weathering and erosion. Sediments are transported to large ancient valleys through small supply channels. A large number of sediments were transported to the southern slope of the Changchang sag through the provenance channel system such as large ancient valleys and slope belts and deposited in the center of the sag. These make up a complete system of large ancient uplifts and submarine fan source-to-sink sedimentary systems. The sedimentary model is a lobed submarine fan controlled by semi-restricted ancient valleys and expansive basins.

#### KEYWORDS

seismic facies, submarine fan, ancient gully, source-to-sink system, sedimentary process

## 1 Introduction

Submarine fans refer to a fan-shaped sedimentary system formed from detritus transported by gravity flow and deposited on continental slopes and abyssal plains (Shanmugam and Moiola, 1988; Richards et al., 1998). The sediment gravity flow has a large transport capacity and distance and can extend hundreds of kilometers from the continental slope to the deep-sea basin (for example, the Bangladesh submarine fan extends over 3000 km) (Talling et al., 2013). Since the concept of submarine fans was introduced, scholars have attempted to establish various depositional models for submarine fans, such as the modern submarine fan model, the ancient submarine fan model, and the comprehensive submarine fan model (Normark, 1978), the ancient submarine fan model (Mutti, 1978), and the comprehensive submarine fan model (Walker, 1978). As research has deepened, scholars have realized that the distribution patterns of submarine fans are complex, due to the interactions between various factors such as sediment type (Reading and Richards, 1994; Gong et al., 2013) and sea-level fluctuations (Pickering and Hiscott, 2015). Differences in structures and ancient landforms (Shultz and Hubbard, 2005; Prélat et al., 2010), including feeder channels, natural levees, lobes, mass transport deposits (MTD), pelagic-hemipelagic sediments, and other sedimentary units, also have significant effects on sedimentation and accumulation (Spychala et al., 2015; Cullis et al., 2018; Liu et al., 2018, 2023). Guided by these submarine fan depositional models, it has been discovered that submarine fan reservoirs are significant enrichment facies for oil, gas, and gas hydrates in passive margin deep-water basins such as those off the coasts of West Africa, the Gulf of Mexico, the North Sea, and offshore Brazil. This indicates that the submarine fan formed by sediment gravity flow has great potential for oil and gas exploration (Piper and Normark, 2001; Weimer et al., 2007; Portnov et al., 2019; Zhang et al., 2019).

Since the beginning of the 21st century, the introduction of high-resolution seismic data processing and interpretation techniques (such as seismic attribute fusion and seismic frequency division analysis) has vastly improved reservoir prediction in submarine fans. Jolly et al. (2016) used 3D seismic data coherent volume stratigraphic slicing technology to precisely describe the geometry of the gravity flow channel of the submarine fan in the Niger Delta Basin, which exhibit characteristics of both lateral and down-dip migration. Howlett et al. (2021) used RGB mixed phase-frequency division to determine the distribution characteristics of miscellaneous reservoir types—such as overbank natural levees and crevasse splays—in the gravity flow channel of the submarine fan in the Kwanza Basin. Especially in areas with no wells and few wells, there is a lack of traditional research data such as drilling, coring and logging. Therefore, it is urgent to utilize high-resolution 3D seismic data to conduct detailed characterization studies of submarine fan reservoirs to reveal their distribution patterns and formation mechanisms.

The Qiongdongnan Basin is one of the significant petroleum-bearing basins in the northern South China Sea, featuring four major source systems: Hainan Island, the Southern Uplift, Vietnam, and the Shenhu Uplift (Cai et al., 2010; Shao et al., 2010). During the deposition period of the Sanya Formation, the source materials from Hainan Island and Vietnam were difficult to input into the Changchang Sag due to transportation distance and the basin's uplift-depression pattern. Previous research has indicated that the Shenhu Uplift in the northern area of the Changchang Sag is elevated, offering abundant source material. A large number of undercut filled erosional channels were found on the uplift, and foreset reflection delta structures have been found in both the first and second members of the Sanya Formation. It is believed that a complete system of source-slope-channel-lobe-apex exists from north to south (Yao et al., 2008). Due to the lack of drilling, the

understanding of the sedimentary environment and provenance of the southern uplift region has been limited for a long time. Submarine fans were relatively developed during the depositional period of the Sanya Formation in the Changchang Sag. During the sedimentary period of the first segment of Sanya Formation, submarine fans were distributed in the southern part of the depression. During the deposition of the second segment of the Sanya Formation, the submarine fans were distributed in the northern part of the sag (Cai et al., 2010). This study used post-stack 3D seismic data to investigate the depositional phases and source-to-sink processes of the submarine fan in the first member of the Sanya Formation in the southern Changchang Sag. The first objective of this study is to determine the internal structure, geometry, and distribution characteristics of the large submarine fan, providing insights for predicting similar submarine fans in other basins and sags. The second objective is to identify the provenance and sedimentary processes of the submarine fan through the analysis of paleogeomorphology and source-to-sink processes. During the deposition period of the first member of the Sanya Formation, the southern uplift zone of the Changchang Sag was locally exposed and subjected to weathering and erosion. Sediments were transported and converged from small feeder channels to large ancient valleys, then delivered through a system of large ancient valleys and slope zones to the slope and central sag area in the southern Changchang Sag, forming a complete depositional system of source-providing ancient uplift and converging submarine fan. This research establishes a geological foundation for hydrocarbon exploration and reservoir analysis in the deep-water area of the Changchang Sag.

## 2 Geologic setting

Located to the southeast of Hainan Island, the Qiongdongnan Basin covers an area of 45,000 km<sup>2</sup>. It is a Cenozoic rifted continental margin oil and gas-bearing basin with a basement composed of pre-Paleogene strata (Li et al., 1998; Wang et al., 2004). The basin is structurally characterized by “north-south zonation”. It is composed of four first-order structural units: the Northern Depression Zone, the Northern Uplift Zone, the Central Depression Zone, and the Southern Uplift Zone (Liao et al., 2012). The Changchang Sag is situated in the east of the Central Depression, bounded by the Shenhu Uplift in the north, the Southern Uplift in the south, and the Baodao Sag in the west. The area extends nearly east-west, covering approximately 10,000 km<sup>2</sup>, with water depths ranging from 1,000 to 2,500 m. The study area is located at the junction of the Changchang Sag and the Southern Uplift, with an area of about 2300 km<sup>2</sup> (Figure 1). The target horizon is the first member of the Sanya Formation.

The Changchang Sag is primarily filled with Cenozoic sediments. It has experienced two tectonic evolution stages: the rifting stage (Paleogene) and the post-rifting stage (Neogene) and has the double-layer structure of the lower fault and the upper depression (Zhao et al., 2010; Ji et al., 2014; Qiu et al., 2014). The maximum sedimentary thickness of the Paleogene strata is nearly 7000 m, including the Eocene and the Oligocene Yacheng and

Lingshui Formations. The maximum thickness of the Neogene strata is nearly 6000 m, including the Miocene Sanya, Meishan, and Huangliu Formations, and the Pliocene Yinggehai Formation. The Quaternary is mainly represented by the Ledong Formation, with a maximum sedimentary thickness of about 1500 m. During the Eocene, the basin primarily experienced lacustrine deposition, while the Oligocene was dominated by fan delta to shallow marine sedimentation. The early to middle Miocene sedimentation was mainly characterized by shallow marine to hemipelagic deposits, whereas the late Miocene to Quaternary sedimentation was dominated by shallow marine to deep marine deposits (Figure 2) (Zhu et al., 2008; Gong et al., 2011; Li et al., 2017).

## 3 Data and method

Because of the absence of boreholes, and the lack of conventional research resources such as cores and well logging data from the study area, this study uses post-stack 3D seismic data. The data cover an area of about 2300 km<sup>2</sup>, with a high signal-to-noise ratio and resolution. The water depth ranges from 1000 m to 2500 m. The bandwidth of the 3D seismic data ranges from 15–55 Hz, with a dominant frequency of 20–45 Hz. The target layer (Sanya Formation submarine fan) has a dominant frequency of approximately 40 Hz. The sampling interval is 2 ms, and the bin size is 25 m × 12.5 m.

This study integrates seismic stratigraphy and sedimentology, applying techniques such as seismic facies analysis, seismic attribute optimization, paleogeomorphology reconstruction, and source-to-sink system analysis. The research investigates the sedimentary processes and genetic mechanisms of the compound submarine fan in the Changchang Sag, Qiongdongnan Basin. A 20 × 20 grid of survey lines were used for tracking, and closed interpretation of the seismic reflection marker beds was carried out at T40, T50, T51 (top of target horizon), T52 (bottom of target horizon), T60, and T100 (Figures 3, 4). The seismic profile is a color variable density profile, where red in-phase axis represent peaks and black in-phase axis represent trough. The types and characteristics of seismic facies were summarized in Figure 3, and the seismic facies division of the whole region is shown in Figure 3G. The interbed attributes were calculated (Figure 4C), revealing the distribution of submarine fan facies (Figure 4D). By combining the interbed attributes with in-phase stratigraphic slices, the seismic attributes of multi-stage RMS amplitudes between T51–T52 were extracted (Figures 5, 6). The paleogeomorphic features before the deposition of T52 were reconstructed based on the sedimentary thickness between T52 and T100 (Figure 7E). According to the characteristics of U-shaped, V-shaped and W-shaped seismic facies of eroded channels, the Channels-ancient gully system was described in detail (Figures 7A, B). Based on the onlap contact relationships between T40, T50, T52, T60, and T100. It was determined that there was some residual denudation on the Southern Uplift Zone during the deposition period of the Sanya Formation (Figure 7D). The seismic reflection characteristics of the composite U-, V-, and W-type feeder channels, combined with a map of the ancient landform, revealed the converging transport channel system for sediments, from numerous small feeder channels to the large ancient gullies in the Southern Uplift Zone (Figure 7E).

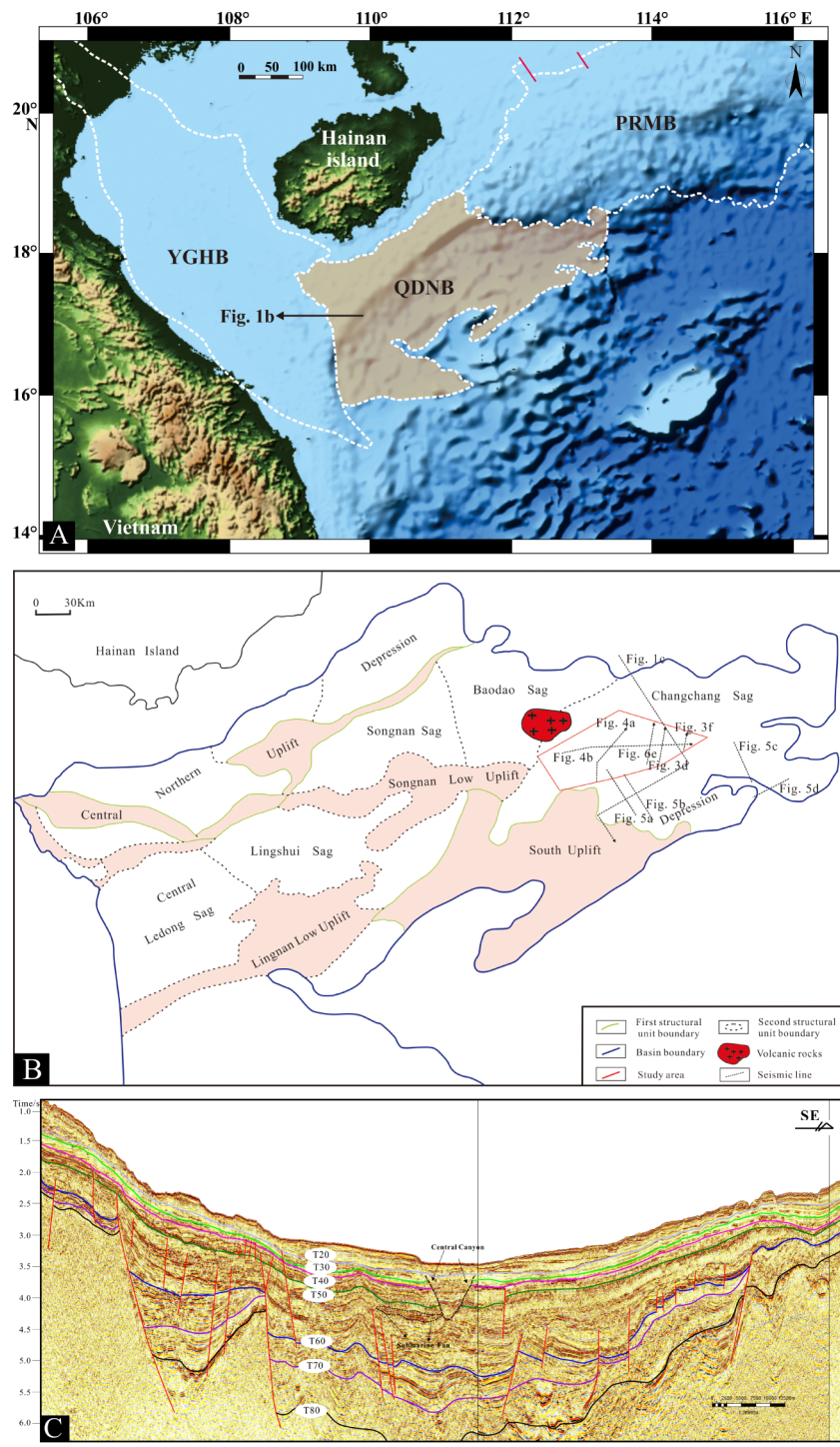


**FIGURE 1** Location of the study area and Seismic profile of Changchang Sag. (A) Location of QDNB; (B) Location of Changchang Sag (Modified from Shi et al., 2019); (C) Seismic section.

## 4 Results

### 4.1 Seismic facies characteristics and genetic interpretation

Seismic facies analysis methods primarily identify seismic facies types based on seismic reflection structure, amplitude, frequency,

and continuity, etc., and then interpret sedimentary environments (Orsolya et al., 2013; Zen et al., 2015; Feng et al., 2020). The 3D seismic data from the Sanya Formation indicates six types of seismic facies: high amplitude parallel sheet reflection, medium amplitude parallel sheet reflection, weak amplitude sub-parallel sheet reflection, high amplitude domain reflection, high amplitude wedge reflection, and divergent channel filling reflection.

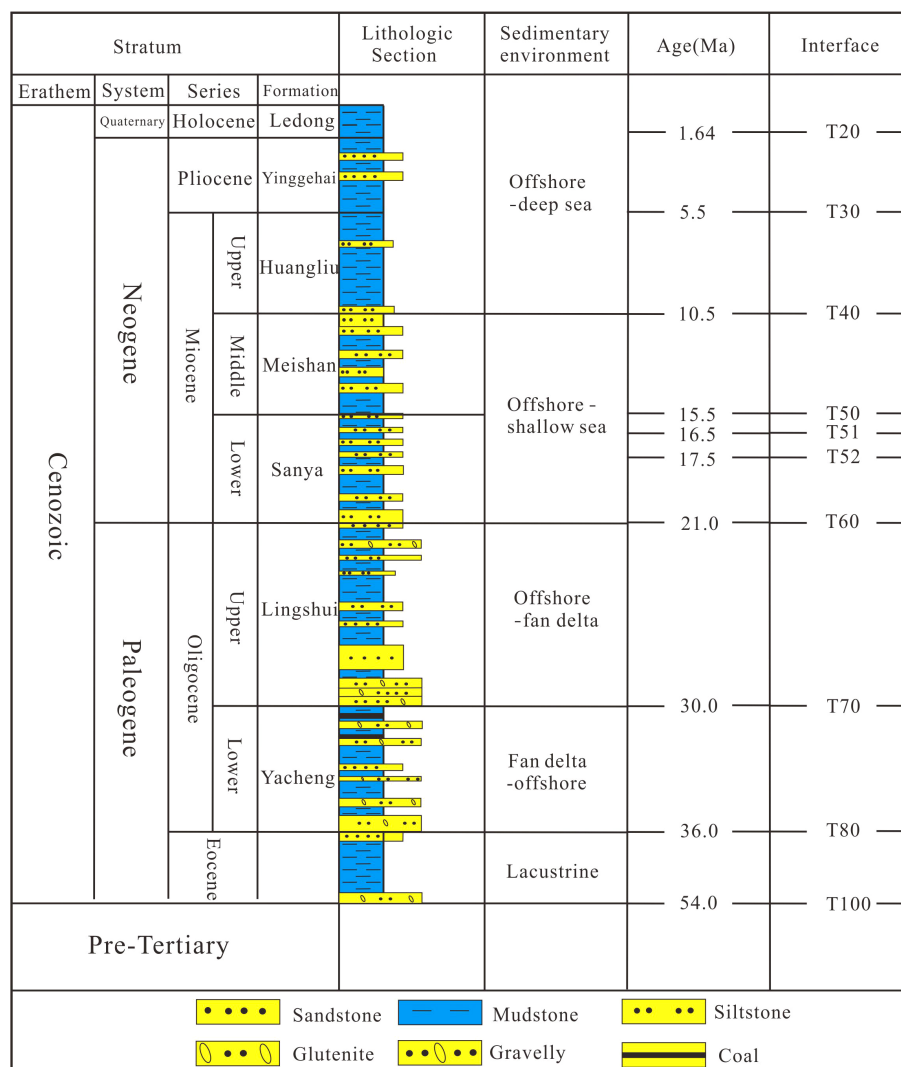


FIGURE 2 Comprehensive stratigraphic column in the Changchang Sag (Modified from Cai, 2017).

### 4.1.1 High amplitude parallel sheet reflection

(1) Description: High amplitude parallel sheet reflection seismic facies are primarily characterized by strong amplitude and high continuity reflections. The upper and lower reflection in-phaseaxis are parallel, the number of high amplitude reflection in-phaseaxis in the lateral direction remains the same, and three to four pairs of strong reflection in-phase axis often occur vertically. The total thickness is approximately 150 m. The reflections from the top have medium-weak amplitude and low continuity, and those from the bottom show weak amplitude sub-parallel sheet reflection (Figure 3A). This type of seismic facies exhibits a fan-shaped distribution on the plane (Figure 3G) and a red-yellow sheet-like distribution on the RMS amplitude attribute graph (Figure 4C).

(2) Interpretation: In deepwater environments, high amplitude, high continuity, and parallel sheet reflection seismic facies are considered as the reflection of the main lobe of a sand-rich submarine fan (Doughty-Jones et al., 2017; Howlett et al., 2021). During the transport of high-energy gravity flow sediments, the

change from steep ancient gullies with continental slope restriction to semi-restricted conditions to broad and flat paleogeomorphology in deep-sea basins causes a significant deceleration of high-energy gravity flows in the deep-sea basin. Coarse-grained sediments are rapidly diffused and deposited, forming sheet-like lobes in the plane. This type of seismic facies exhibits a conformable contact with the underlying strata, indicating weak sediment erosion and primarily unloading deposition.

### 4.1.2 Medium amplitude parallel sheet reflection

(1) Description: Medium amplitude parallel sheet reflection seismic facies are characterized by medium amplitude and moderate continuity reflections. The upper and lower reflection in-phaseaxis are approximately parallel. Laterally, the number of medium-amplitude reflection in-phaseaxis remains stable. Vertically, 3-4 pairs of in-phaseaxis are developed. Toward the deep-sea basin, there is a gradual transition from weak amplitude at the base to increasing reflection characteristics upwards (Figure 3B). This kind of seismic

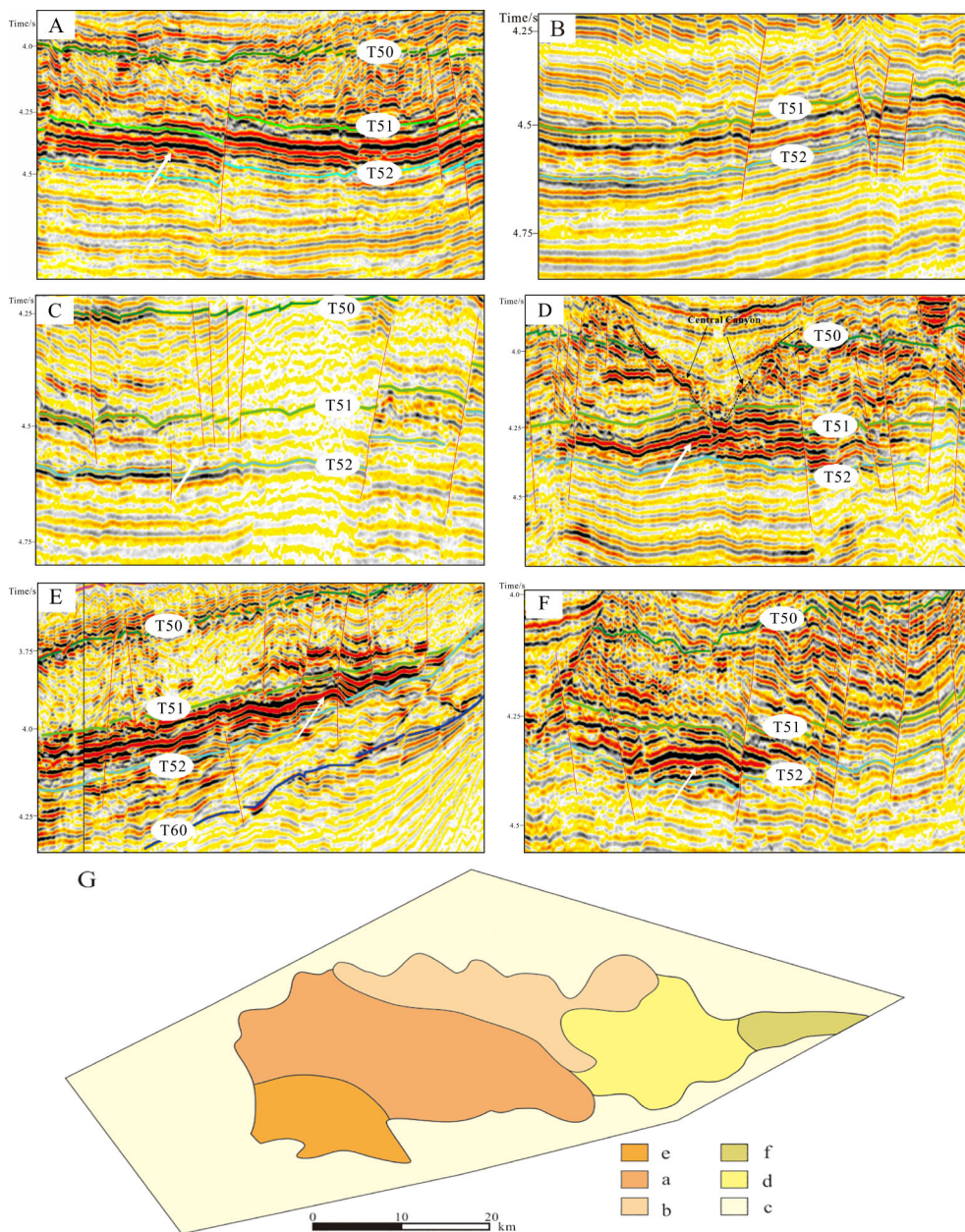


**FIGURE 3** Reflection characteristics of the seismic facies of the Sanya Formation submarine fan in the Changchang Sag (The white arrows indicate the locations of typical seismic facies). (A) High amplitude parallel sheet reflection; (B) Medium amplitude parallel sheet reflection; (C) Weak amplitude sub-parallel sheet reflection; (D) High amplitude domal reflection; (E) High amplitude wedge reflection; (F) Divergent filling reflection of channel; (G) Plane distribution of seismic facies.

facies shows girdle-pattern distribution at the edges of the fan in the plane (Figure 3G), and a yellow-light blue girdle-pattern distribution on the RMS amplitude attribute graph (Figure 4C).

(2) Interpretation: In deepwater environments, medium amplitude, high continuity, and parallel sheet reflection seismic facies are considered to be the reflection of the distal end lobe of a submarine fan (Kane and Pontén, 2012; Soutter et al., 2019). Coarse-grained sediments in high-energy gravity flow slow down as they reach the open, flat, low-lying areas of the abyssal basin and are swiftly unloaded. However, turbidite sediments, with lower flow velocity, continue to flow from the main lobe of the fans towards the

sides of the abyssal basin, with the flow velocity gradually reducing until stagnation sets in, forming distal end lobes with distinctive girdle deposition patterns.

### 4.1.3 Weak amplitude sub-parallel sheet reflection

(1) Description: Weak amplitude sub-parallel sheet reflection seismic facies are characterized by weak amplitude and low continuity reflections. The upper and lower reflection in-phase axis are approximately parallel or wave-like in distribution. Laterally, the number of weak amplitude reflection in-phase axis

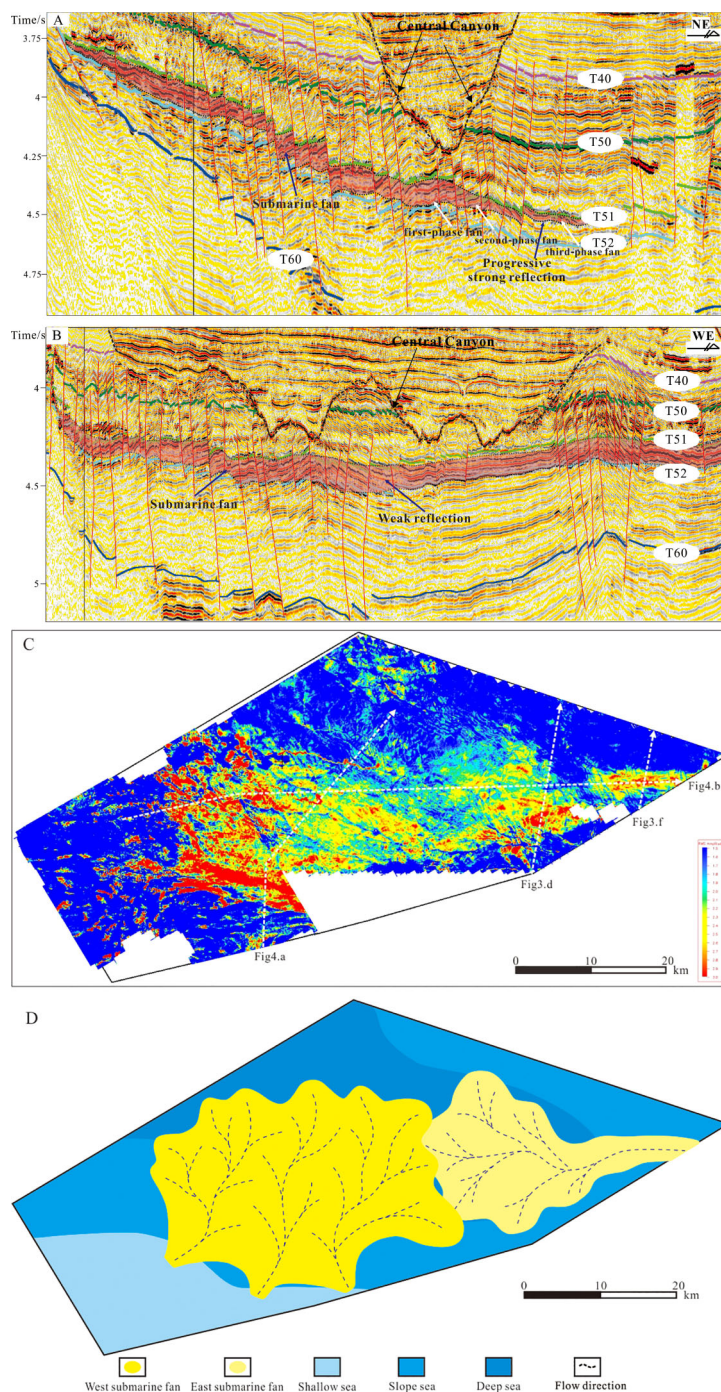
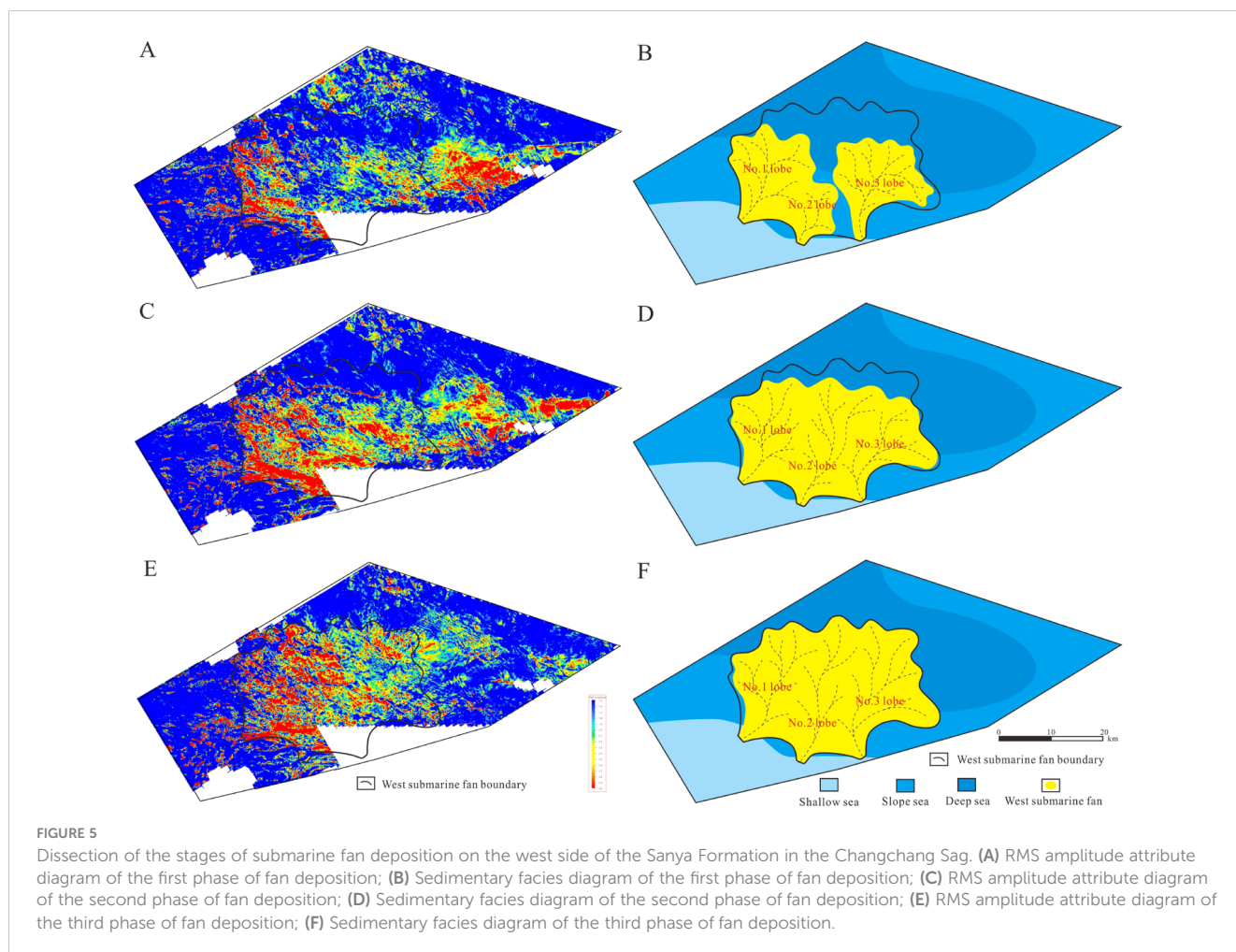


**FIGURE 4**  
 Geometric shape and plane distribution of the submarine fan in the Sanya Formation in the Changchang Sag. (A) Nearly north-south seismic profile of the west fan; (B) Nearly east-west seismic profile of the submarine fan; (C) RMS amplitude attribute map; (D) Sedimentary facies of the submarine fan.

remains generally unchanged. Toward the deep-sea basin, these facies often transition from strong or medium amplitude parallel sheet reflection seismic facies to weak amplitude sub-parallel sheet reflection seismic facies. Vertically, they are primarily distributed at the top and bottom of strong or medium amplitude parallel sheet reflection seismic facies (Figure 3C). It is found in the peripheral areas of fans in the plane (Figure 3G) and shows as a blue area on the RMS amplitude attribute graph (Figure 4C).

(2) Interpretation: In deep-water environments, weak-amplitude, low-continuous, subparallel sheet-reflection seismic facies are often considered semi-deep-abyssal mudstone deposits (Spychala et al., 2015; Cullis et al., 2018). Although the semi-abyssal-deep sea floor has no wave action, it is still accompanied by ocean currents or bottom currents with very low deposition rates. A large amount of terrigenous muddy sediments are transported in a suspended manner and are slowly deposited in



the calm semi-deep sea-deep sea together with the remains of plankton and plants.

#### 4.1.4 High amplitude domal reflection

(1) Description: High amplitude domain reflection is a seismic facies with high amplitude and high continuity. The top and bottom reflection boundaries are clear: the top reflection boundary is a medium-strong wave peak reflection and the bottom boundary is an approximately parallel-flat, medium-strong wave trough reflection. The strong reflection profile is hummocky and lentoid, with the length of strong reflection in-phase axis gradually increasing from bottom to top, indicating bidirectional download (Figure 3D). This kind of seismic facies is located at the fan root in the plane (Figure 3G) and is represented as a red-yellow broom-shaped area on the RMS amplitude attribute graph (Figure 4C).

(2) Interpretation: In deep-water environments, seismic facies with strong amplitude and continuous mound reflection are often considered fan-root deposits of sand-rich submarine fans (Doughty-Jones et al., 2017; Howlett et al., 2021). During the transport of high-energy gravity flow sediments from the continental slope to the deep-sea basin, the transition from slope-restricted and semi-restricted ancient gullies to flat deep-sea basins slows the transport speed of coarse-grained sediments, leading to rapid diffusion and unloading

deposition. Multi-phase gravity flow sediments migrate laterally, stack vertically, and finally form fan root deposits, longitudinally hummocky and broom-shaped in the plane.

#### 4.1.5 High amplitude wedge reflection

(1) Description: High amplitude wedge reflection seismic facies are characterized by strong amplitude and high continuity reflections with clear top and bottom reflection interfaces. Moving from the slope to the deep-sea basin, the number of strong reflection in-phase axis gradually increases from 1 pair to 3-4 pairs. The overall shape is divergent or wedge-shaped, and it exhibits onlap contact with the underlying strata (Figure 3E). This type of seismic facies is at the fan root in the plane (Figure 3G), and shows as a red area on the RMS amplitude attribute graph (Figure 4C).

(2) Interpretation: In deepwater environments, high-amplitude, high-continuity wedge reflection seismic facies is generally deemed to represent the fan-root deposits of sand-rich submarine fans (Doughty-Jones et al., 2017; Howlett et al., 2021). The early high-energy gravity flow sediments diffused and unloaded rapidly in the transition zone connecting the continental slope to the deep-sea basin. When the supply of gravity flow sediments was sufficient and the multi-phase gravity flow occurred frequently, the restricted-semi-restricted ancient valleys on the continental slope were very

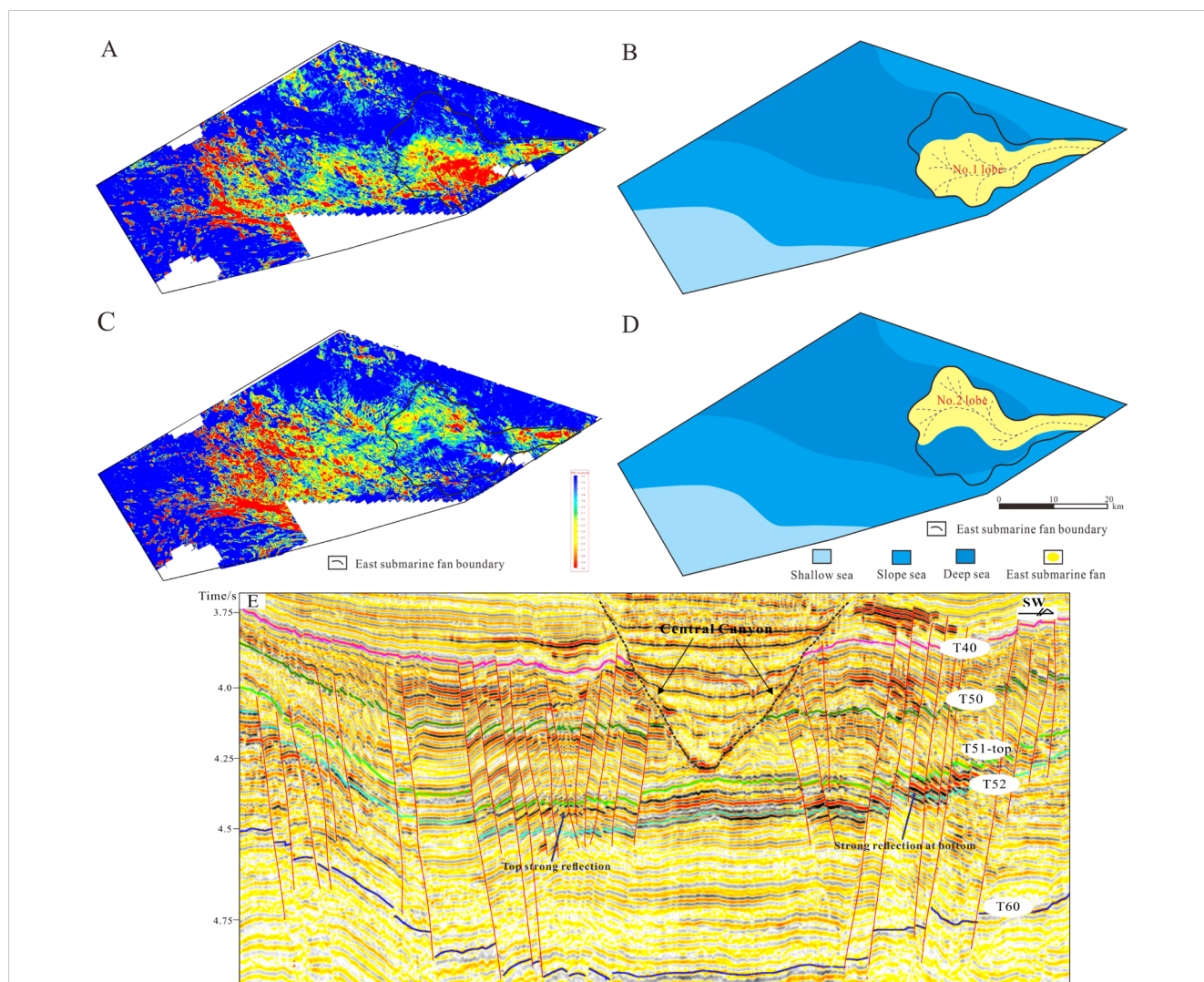


**FIGURE 6**  
 Dissection of the depositional stage of the submarine fan in the east of the Sanya Formation in the Changchang Sag. (A) RMS amplitude attribute diagram of the first phase of fan deposition; (B) Sedimentary facies diagram of the first phase of fan deposition; (C) RMS amplitude attribute diagram of the second phase of fan deposition; (D) Sedimentary facies diagram of the second phase of fan deposition; (E) Near north-south oriented seismic profile of the eastern fan.

fast. Filled by gravity flow sediments, the middle and late gravity flow sediments continued to be rapidly unloaded and deposited along the continental slope on top of the early sediments, forming the wedge-shaped reflection feature of the upper retrograde supertype.

#### 4.1.6 Divergent filling reflection of channel

(1) Description: Divergent filling reflection of channel is a seismic facies with high amplitude and high continuity. The top and bottom reflection boundaries are clear. The profile shape is flat-topped, convex-bottomed, or lenticular. From the bottom to the top, the strong reflection in-phase axis gradually become longer, representative of divergent onlap (Figure 3F). This kind of seismic facies are connected to the fan root in the plane. It is closer to the source direction (Figure 3G) and its RMS amplitude attribute shows as a narrow red-yellow strip (Figure 4C).

(2) Interpretation: In deepwater environments, divergent filled reflection seismic phases in channels are considered as sand-rich feeder channels (Mayall et al., 2006; Janocko et al., 2013; Howlett et al., 2021). Low-sinuosity feeder channels may be formed by high-energy gravity flows with predominantly laminar flow, and high-sinuosity feeder channels may be formed by low-energy gravity flows with dominantly turbulent flow.

### 4.2 Distribution characteristics and depositional stages of submarine fans

#### 4.2.1 Distribution characteristics of submarine fans

Seismic facies analysis indicates that on the plane of the Sanya Formation submarine fan in the Changchang Depression, the filling

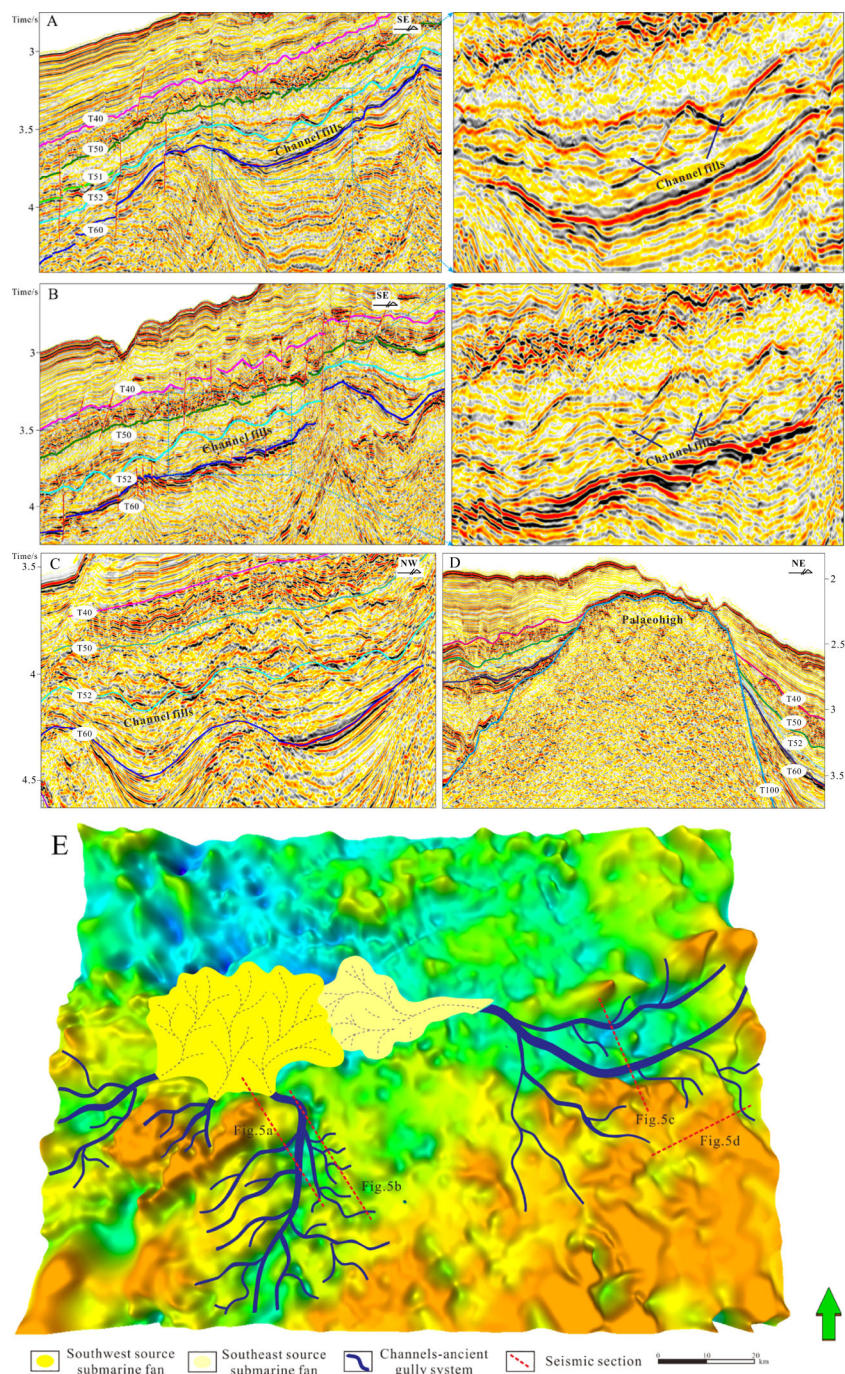


FIGURE 7

Source-to-sink system of the submarine fan in the Sanya Formation in the Changchang Sag. (A) W- and V-type feeder channels in the fan on the west side; (B) U-type feeder channel in the fan on the west side; (C) Feeder channel in the fan on the east side; (D) Denuded residual paleo-uplift in the Southern Uplift Zone; (E) Overlay of the ancient landform and the source-to-sink system of the submarine fan, showing the area during the deposition period of the first member of the Sanya Formation.

reflections successively diverge from east to west (Figures 3F-G), high amplitude domain reflection (Figures 3D, G), medium amplitude parallel sheet reflection (Figures 3B, G), high amplitude parallel sheet reflection (Figures 3A, G), and high amplitude wedge reflection (Figures 3E, G). In general, the reflections are strong at both the east and west ends but comparatively weak in the middle (Figure 3G). Seismic attribute analysis indicates that the plane of the

fan body exhibits a long and strip-shaped distribution, with the eastern part being the narrowest, the central part gradually widening, and the western part being the widest. The length of the fan body is about 70 km and the area is about 1100 km<sup>2</sup>. It looks like an elongated lobe from east to west (Figure 4C).

Comparison with seismic profiles oriented nearly north-south reveals that the eastern fan body profiles exhibit a lens-shaped

morphology with a flat top and a convex bottom (Figures 3F, 4C) and a mound-shaped morphology with a flat bottom and a convex top (Figures 3D, 4C). The overall geometry features thick middle and thin wings; the profile morphology of the western fan body exhibits wedge-shaped reflections, and the strong reflection in-phase axis gradually thins from south to north. The number of in-phase axis decreases gradually from 4-5 to 1 (Figure 4A). The fan is thick in the south (thickest 170 ms) and thin in the north (thinnest 25 ms).

#### 4.2.2 Depositional stages of the progradational submarine fan in the west

The RMS amplitude attribute (Figure 4C) and ancient landform diagrams (Figure 7E) show that there are three large strip-shaped ancient gullies in the southwest of the uplift area. These gullies are connected with the fan root of the western submarine fan, suggesting that the western part of the fan may have had multiple supply channels. On the nearly north-south profile of the fan on the west side, the target horizon between T52-T51 gradually transitions from middle-weak amplitude to high amplitude in the extension direction of the basin, showing the obvious strong reflection characteristics typical of progradation (Figure 4A). Based on the changes in the number of strong reflection in-phase axis and the pinch-out characteristics of strong reflection in-phase axis (Figure 4A), along with the planar distribution characteristics of seismic attributes, the western submarine fan is characterized as having three progradational depositional phases.

The black circle on the RMS amplitude attribute diagram defines the distribution range of the entire west side of the fan. It clearly shows that the high amplitude seismic attribute of the first stage of fan deposition is mainly in the southern slope (Figure 5A). No. 1 lobe is connected to No. 2 lobe, with an area of 339.5 km<sup>2</sup>, while No. 3 lobe covers an area of 232.1 km<sup>2</sup>. The total area of the three lobes is 571.6 km<sup>2</sup> (Figure 5B). The distribution range of strong amplitude seismic attributes in the second phase fan is significantly larger than that of the first phase fan, covering an area of 760.3 km<sup>2</sup> (Figure 5C), but the sediments did not fill the entire fan area. All three lobes extended to the basin (Figure 5D), with the progradation extent of No. 2 lobe being the greatest. The distribution range of the high amplitude seismic attribute of the third stage of fan deposition is the largest (Figure 5E). During this period, the distribution range of sediments was the largest (905 km<sup>2</sup>), filling the entire fan area. No. 1 lobe spread to the northwest of the basin, No. 2 lobe continued to prograde northwards, and No. 3 lobe spread to the northeast of the basin (Figure 5F).

#### 4.2.3 Depositional stage of eastern lateral accretion-type submarine fan

The RMS amplitude attribute (Figure 4C) and ancient landform (Figure 7E) diagrams show a large banded ancient gully in the southeast of the uplift area. It is connected with the fan root on the east side of the submarine fan. It is inferred that this gully was the sole supply system for the eastern part of the fan. The strong reflective in-phase axes of the southern side of the submarine fan are distributed at the bottom, gradually weakening from bottom to

top, while on the northern side, the strong reflective in-phase axes are distributed at the top, gradually strengthening from bottom to top. Based on the differing characteristics of the strong reflective in-phase axes on the southern and northern sides (Figure 6E), combined with the plane distribution characteristics of seismic attributes. It can be seen that the eastern submarine fan is a two-phase lateral depositional stage.

The range delineated by the black line on the root mean square amplitude attribute map corresponds to the distribution range of the entire eastern compound fan body. It is evident that the strong amplitude seismic attributes of the first-phase fan body are mainly distributed on the southern side (271.1 km<sup>2</sup>) (Figure 6A), and the sediments do not completely fill the entire distribution range of the fan body. During this period, the No. 1 lobe was oriented nearly east-west, and all of the lobes were on the west side of the fan. A low-sinuosity feeder channel can be observed as a long strip on the RMS amplitude attribute diagram (Figures 6A, B). Following the first phase, fan deposition migrated laterally northwards (Figure 6C), and the medium-high amplitude seismic attribute of the second phase of fan deposition is visible in the north (249.1 km<sup>2</sup>), with the sediments still not filling the entire fan area. During this period, the No. 2 lobe was also oriented nearly east-west on the west side of the fan, with sediments continuously supplied through the low-sinuosity feeder channel of the No. 1 lobe (Figures 6C, D).

## 5 Discussion

### 5.1 The evidence of two sets of submarine fans

Source-to-sink systems have always been a popular research area for scholars both domestically and internationally. The main objective is to integrate the entire sedimentary process of sediment from the erosion zone, transport basin, and towards the sedimentary basins into a system that ranges from “source” to “sink”. Then study the dynamic process of the earth’s surface and its control on the deposition process (Lin et al., 2015; Romans et al., 2016; Bernhardt et al., 2017). Tectonic activity, paleoclimate, ancient landforms, and sea-level changes are all key factors influencing the evolution of source-to-sink systems (Fildani et al., 2016; Hessler et al., 2018; Lin et al., 2021). Detrital zircon geochronology and heavy mineral composition analysis are effective techniques for source-to-sink analysis (Liu et al., 2020, 2022) However, no drilling has been conducted in the study area, and traditional research data such as core samples and well logs are lacking. Therefore, we primarily used post-stack 3D seismic data and employed techniques such as seismic facies analysis, optimal selection of seismic attributes, and paleogeographic reconstruction to study the source-to-sink processes of the submarine fans.

By analyzing the geometric characteristics of the submarine fan of Sanya formation in Changchang sag, it is found that this set of fan bodies is not a single-source submarine fan. Instead, it may be a composite of two submarine fans from the southwest and southeast

sources (Figure 4D). The reasons for this conclusion are as follows. ① The seismic facies overall exhibit strong reflections at the eastern and western ends, with relatively weak reflections in the middle, forming a planar distribution pattern (Figure 3G). ② On the nearly east-west seismic profile (Figure 4B), there are strong reflections at the east and west ends, and an obvious weak reflection area in the middle. ③ The RMS amplitude attribute map also shows an apparent weak reflection strip in the middle of the fan (Figure 4C). ④ On the near north-south cross-section, the geometric features of the fan bodies on the east and west sides show significant differences. The fan body on the east side exhibits a reflection characteristic that thickens in the middle and tapers towards the wings. In contrast, the fan body on the west side shows a reflection characteristic where it gradually thickens towards the south, thins towards the north, and tapers off.

## 5.2 Southwest provenance submarine fan

From a sedimentary period paleogeographic map of the Sanya Formation, it can be observed that the southern side of the Changchang Sag constitutes a southern uplifted area, generally displaying a characteristic of being higher in the south and lower in the north. Within this uplifted area, multiple residual eroded ancient uplifts have been identified, which correspond to the orange-yellow regions on the paleogeographic map (Figure 7D, E). During the deposition period of the Sanya Formation, a specific region in the southern uplift area was long exposed to water, undergoing weathering and erosion. This provides provenance conditions for the submarine fan deposition in the deep water area on the southern side of the Changchang Sag.

There are three large banded ancient gullies in the southwest of the uplift area, oriented generally NNE (Figure 7E). The seismic facies in the area of the gullies show that feeder channels are relatively plentiful, mostly U-shaped, V-shaped, and composite W-shaped. The interiors of the feeder channels are filled with vertically or laterally stacked sediments (Figures 7A, B). These feeder channels are mainly distributed along both sides of the ancient valley and converge towards the ancient valley. They provide favorable pathways for sediment transport. Three large ancient valleys passed through the southwest uplift area and merged into the Changchang sag. Their distribution positions were connected to the fan root of the fan body on the west side (Figure 7E). This is the most direct evidence of the southwest provenance submarine fan.

## 5.3 Southeast provenance submarine fan

In the southeastern part of the uplifted area, a large banded ancient valley can be observed, mainly exhibiting a near east-west distribution (Figure 7E). Seismic facies analysis of the distribution area of the ancient valley reveals that the area's feeder channels are also well developed, generally U-, V-, and composite W-shaped. The channels locally show evidence of both vertical and lateral migration and their interiors are filled with vertically or laterally stacked

sediments (Figure 7C). The small feeder channels are distributed along both sides of the ancient valley, converging into the ancient valley, providing a favourable supply channel for the transportation of sediments. The large ancient valley runs through the uplifted southeast region, flowing into the Changchang Sag. Its position links to the eastern fan root of the fan body (Figure 7E). This is the most direct evidence of the southeastern source submarine fan.

## 5.4 Sedimentary model of submarine fans

Ancient landforms, gullies, and shelf-break belts are significant factors affecting the source-to-sink supply systems of shelf-margin submarine fans (Gong et al., 2013; Romans et al., 2016; Bernhardt et al., 2017). Domestic scholars have studied the source-to-sink systems of basins such as South Sumatra, Bohai Bay, and Pearl River Estuary. It was found that synsedimentary faults, ancient valleys and ancient landforms jointly controlled the sedimentary evolution, geometry and distribution direction of submarine fans (fan deltas) (Hu et al., 2020; Zhao et al., 2020; Feng et al., 2021). During the deposition of the Sanya Formation, the southern side of the Changchang Sag was the Southern Uplift Zone (the orange-yellow area in Figure 7E), which had a much larger area than the sag itself. The subsidence center of the sag was located northwest of the basin (the blue area in Figure 7E). In the southern uplifted area, specific regions underwent prolonged weathering and erosion during this time (Figure 7D). Sediments were carried from small feeder channels to large ancient valleys, where a substantial amount of sediment was transported through the large ancient valleys and sloping zones, among other pathways, to be deposited from the southern slope of the Changchang Sag to the depression center (Figure 7E). This constituted a complete system of large ancient uplifts and submarine fan source-to-sink sedimentary systems (Figure 8). The southwest-prograding submarine fan exhibits a near north-south orientation, primarily being fed by three large, belt-like ancient valleys transporting sediments. In the near-north-south seismic profile, the in-phase axis gradually transitions from the middle-weak amplitude to the strong amplitude from bottom to top and extends toward the center of the basin. This submarine fan exhibits distinct characteristics of three phases of progradation deposition. The southeastern provenance lateral accretion type submarine fan is distributed in a nearly east-west direction. It is mainly transported by a single large strip of ancient valleys. RMS amplitude property analysis shows that it extends towards the center of the basin. This set of submarine fans is filled with two-phase lateral depositional sediments. Two sets of submarine fans converge in the Changchang sag basin. As a whole, it is a coupled deposition of prograde and lateral submarine fans, controlled by semi-restricted ancient valleys and open basins (Figure 8). Its formation mechanism may be related to factors such as the long-term exposure and weathering of large ancient uplifts providing sediment sources, paleogeomorphology controlling channels and sand, seasonal rainfall and floods inducing large sediment transport, and the open topography of the depression area facilitating sediment unloading. However, more evidence is needed to confirm these mechanisms in future research.

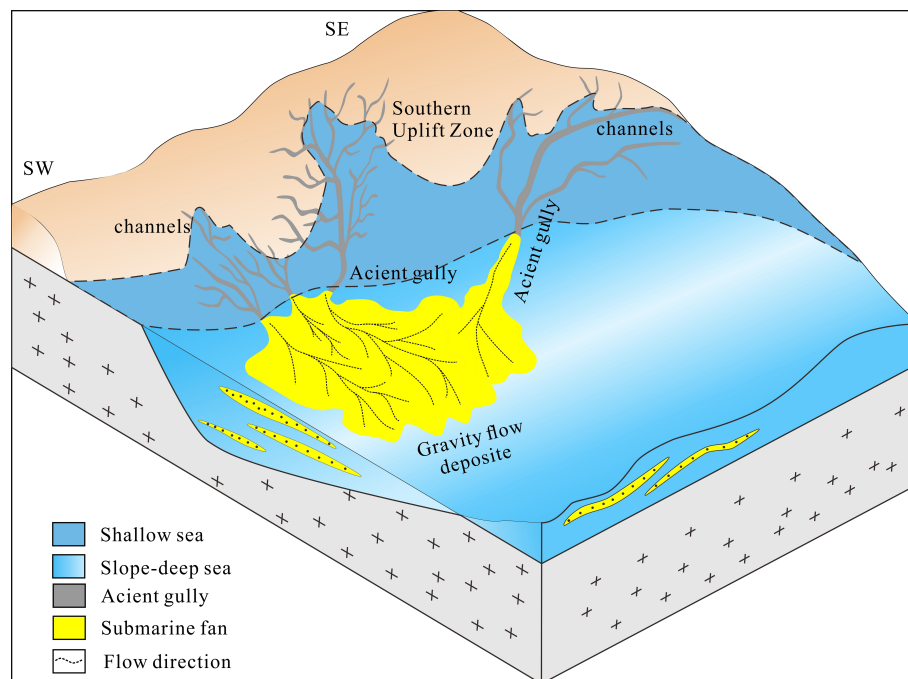


FIGURE 8

Sedimentary model of the progradational and lateral accretion submarine fan in the Sanya Formation in the Changchang Sag.

## 6 Conclusions

(1) Six types of seismic facies were distinguished in the analysis of the depositional period of the Sanya Formation, in the Changchang Sag in the Qiongdongnan Basin, and their geneses determined: a) the seismic facies of the main lobe of the sand-rich submarine fan in the formation displays high amplitude, high continuity, and parallel sheet reflection; b) the distal end lobe of the fan shows medium amplitude, medium continuity, and parallel sheet reflection; c) the hemipelagic-pelagic mudstone exhibits weak amplitude, low continuity, and sub-parallel sheet reflection; d) the fan root shows high amplitude, high continuous domain in reflection or high amplitude high continuous wedge reflection; and e) the feeder channel displays divergent filling channel reflection.

(2) According to its geometric features, seismic facies features, and RMS amplitude attributes, the submarine fan of the Sanya Formation can be divided into two parts, one with a southwestern provenance and the other with a southeastern provenance. The submarine fan of southwest provenance is distributed in a nearly north-south direction. It is mainly transported by three large strip-shaped ancient valleys, extending to the center of the basin. The sedimentary filling is characterized by three-phase progradation. The submarine fan of southeastern provenance is distributed in a nearly east-west direction. It is mainly transported by a single large strip-shaped ancient valley extending to the center of the basin. The sedimentary filling is characterized by two-phase lateral accumulation.

(3) During the deposition of the Sanya Formation, the southern side of the Changchang Sag belongs to the southern uplift zone. The subsidence centre of the depression is located in the northwest part of the basin. Local areas of the southern uplift zone were exposed to

weathering and denudation for a long time during this period. Sediments are transported and gathered in large ancient valleys by small supply channels. A large number of sediments were transported to the southern slope of the Changchang sag through the provenance channel system such as large ancient valleys and slope belt and finally deposited in the center of the sag. This constituted a complete system of large ancient uplifts and submarine fan source-to-sink sedimentary systems. As a whole, it is a coupled deposition of prograde and lateral submarine fans, controlled by semi-restricted ancient valleys and open basins.

## Data availability statement

The raw data supporting the conclusions of this article will be made available by the authors, without undue reservation.

## Author contributions

CF: Data curation, Funding acquisition, Resources, Writing – original draft, Writing – review & editing. GF: Investigation, Supervision, Writing – review & editing. ZY: Data curation, Formal analysis, Investigation, Writing – review & editing. XY: Formal analysis, Investigation, Writing – review & editing. XS: Conceptualization, Data curation, Formal analysis, Writing – review & editing. WL: Investigation, Supervision, Validation, Writing – review & editing. HQ: Project administration, Supervision, Visualization, Writing – review & editing. QZ: Data curation, Project administration, Visualization, Writing – review & editing. XW: Methodology, Project administration, Visualization, Writing – review & editing.

## Funding

The author(s) declare financial support was received for the research, authorship, and/or publication of this article. This study was supported by National Natural Science Foundation of China (Grant No. 42372154), National Science and Technology Major Project (Grant No. 2016ZX05026-007-007), Natural Science Basic Research Plan in Shaanxi Province of China (Grant No. 2017JM4013; 2020JQ-798), and the Scientific Foundation of Geology Department, Northwest University.

## Acknowledgments

We gratefully acknowledge the editor for careful editorial handling and the two reviewers for reviewing this manuscript. Thanks to graduate students Fenglian Zhang and Daming Li for drawing figures.

## References

- Bernhardt, A., Schwanghart, W., Hebbeln, D., Stuut, J. B. W., and Strecker, M. R. (2017). Immediate propagation of deglacial environment change to deep-marine turbidite systems along the Chile convergent margin. *Earth Planetary Sci. Letters*. 473, 190–204. doi: 10.1016/j.epsl.2017.05.017
- Cai, J. (2017). Sedimentary facies of neogene sanya formation in changchang sag, qiongdongnan basin. *Lithologic Reservoirs*. 29, 46–54. doi: 10.3969/j.issn.1673-8926.2017.05.006
- Cai, J., Li, G. L., Gan, H. J., and Liao, J. H. (2010). Seismic Inversion and Prediction of Sand Bodies in Boundary Fault Zones of Nanyang Sag. *Lithologic Reservoirs*. 22 (2), 99–102. doi: 10.3969/j.issn.1673-8926.2010.02.018
- Cullis, S., Colombera, L., Patacci, M., and McCaffrey, W. D. (2018). Hierarchical classifications of the sedimentary architecture of deep-marine depositional systems. *Earth-Science Rev.* 179, 38–71. doi: 10.1016/j.earscirev.2018.01.016
- Doughty-Jones, G., Mayall, M., and Lonergan, L. (2017). Stratigraphy, facies, and evolution of deep-water lobe complexes within a salt-controlled intraslope minibasin. *AAPG Bulletin*. 101, 1879–1904. doi: 10.1306/01111716046
- Feng, C. J., Sun, M. S., Liu, C. Y., Deng, X. L., Xue, Y. Z., and Dong, L. (2020). Seismic sedimentary characteristics and filling structure of the Upper Triassic Yanchang Formation, Ordos Basin, China. *Interpretation*. 8, T259–T274. doi: 10.1190/int-2019-0138.1
- Feng, C. J., Yao, X. Z., Yang, H. Z., Li, D. M., and Sun, M. S. (2021). Source-to-sink system and sedimentary model of progradational fan delta controlled by restricted ancient gully: an example in the enping formation in the southern baiyun sag, pearl river mouth basin, northern south China sea. *Acta Geologica Sinica-English Edition*. 95, 232–247. doi: 10.1111/1755-6724.14627
- Fildani, A., Mckay, M. P., Stockli, D., Clark, J., Dykstra, M. L., Stockli, L., et al. (2016). The ancestral Mississippi drainage in the late Wisconsin deep-sea fan. *Geology*. 44, 479–482. doi: 10.1130/G37657.1
- Gong, C. L., Wang, Y. M., Zhu, W. L., Li, W. G., and Xu, Q. (2013). Upper Miocene to Quaternary unidirectionally migrating deep-water channels in the Pearl River mouth Basin, northern South China Sea. *AAPG Bulletin*. 97, 285–308. doi: 10.1306/07121211159
- Gong, C. L., Wang, Y. M., Zhu, W. L., Li, W. G., Xu, Q., and Zhang, J. M. (2011). The central submarine canyon in the Qiongdongnan Basin, northwestern South China Sea: Architecture, sequence stratigraphy, and depositional processes. *Mar. Petroleum Geology*. 28, 1690–1702. doi: 10.1016/j.marpetgeo.2011.06.005
- Hessler, A. M., Covault, J. A., Stockli, D. F., and Fildani, A. (2018). Late Cenozoic cooling favored glacial over tectonic controls on sediment supply to the western Gulf of Mexico. *Geology*. 46, 995–998. doi: 10.1130/g45528.1
- Howlett, D. M., Gawthorpe, R. L., Ge, Z. Y., Rotevatn, A., and Jackson, C. A. L. (2021). Turbidites, topography and tectonics: Evolution of submarine channel-lo be systems in the salt-influenced Kwanza Basin, offshore Angola. *Basine Res.* 33, 1076–1110. doi: 10.1111/bre.12506
- Hu, W. Y., Luo, W., Huang, C., Deng, G. J., Fu, D. W., and Lei, X. (2020). Characteristics of Dongsha movement in Qiongdongnan basin and its petroleum geo-logical significance. *China Offshore Oil and Gas*. 32 (3), 20–32. doi: 10.11935/j.issn.1673-1506.2020.03.003
- Janocko, M. N. W. H. S. W. M., Nemeč, W., Henriksen, S., and Warchot, M. (2013). The diversity of deep-water sinuous channel belts and slope valley-fill complexes. *Mar. Petroleum Geology*. 41, 7–34. doi: 10.1016/j.marpetgeo.2012.06.012
- Ji, M., Zhang, G. C., Yang, H. Z., Yang, D. S., and Li, C. L. (2014). Structural pattern and evolution of eastern sag belt, in deep-water area of Qiongdongnan Basin. *Mar. Geology Frontiers*. 30, 26–35. doi: 10.16028/j.1009-2722.2014.09.015
- Jolly, B. A., Lonergan, L., and Whittaker, A. C. (2016). Growth history of fault-related folds and interaction with seabed channels in the toe-thrust region of the deep-water Niger delta. *Mar. Petroleum Geology*. 70, 58–76. doi: 10.1016/j.marpetgeo.2015.11.003
- Kane, I. A., and Pontén, A. S. M. (2012). Submarine transitional flow deposits in the Paleogene Gulf of Mexico. *Geology*. 40, 1119–1122. doi: 10.1130/G33410.1
- Li, S. T., Lin, C. S., Zhang, Q. M., Yang, S. G., and Wu, P. K. (1998). The multiple rifting dynamic processes of the continental marginal basin, north of the South China Sea and tectonic event from 10 Ma. *Chin. Sci. Bulletin*. 43, 797–810. doi: 10.1007/bf03182877
- Li, C., Lv, C. F., Chen, G. J., Zhang, G. C., Ma, M., Shen, H. L., et al. (2017). Source and sink characteristics of the continental slope-parallel central canyon in the Qiongdongnan Basin on the northern margin of the South China Sea. *J. Asian Earth Sci.* 134, 1–12. doi: 10.1016/j.jseas.2016.10.014
- Liao, J. H., Wang, H., Sun, Z. P., Zhang, D. J., Xiao, J., Sun, M., et al. (2012). Tectonic evolution and its controlling on sequence pattern of Chang-chang Sag, deep water area of Qiongdongnan Basin, South China Sea. *J. Cent. South Univ. (Science Technology)*. 43, 3121–3132.
- Lin, C. S., Xia, Q. L., Shi, H. S., Zhou, X., and Zhou, X. H. (2015). Geomorphological evolution, source to sink system and basin analysis. *Earth Sci. Frontiers*. 22, 9. doi: 10.13745/j.esf.2015.01.002
- Lin, C., Zhang, J. J., Wang, X. X., Huang, T. L., Zhang, B., and Fan, Y. S. (2021). Himalayan Miocene adakitic rocks, a case study of the Mayum pluton: Insights into geodynamic processes within the subducted Indian continental lithosphere and Himalayan mid-Miocene tectonic regime transition. *GSA Bulletin*. 133, 591–611. doi: 10.1130/B35640.1
- Liu, E. T., Chen, S., Yan, D. T., Deng, Y., Wang, H., Jing, Z., et al. (2022). Detrital zircon geochronology and heavy mineral composition constraints on provenance evolution in the western Pearl River Mouth basin, northern south China sea: A source to sink approach. *Mar. Petroleum Geology*. 145, 105884. doi: 10.1016/j.marpetgeo.2022.105884
- Liu, Q., Kneller, B., Fallgatter, C., Valdez Buso, V., and Milana, J. P. (2018). Tabularity of individual turbidite beds controlled by flow efficiency and degree of confinement. *Sedimentology*. 65, 2368–2387. doi: 10.1111/sed.12470
- Liu, E. T., Wang, H., Feng, Y. X., Pan, S. Q., Jing, Z. H., Ma, Q. L., et al. (2020). Sedimentary architecture and provenance analysis of a sublacustrine fan system in a half-graben rift depression of the South China Sea. *Sedimentary Geology*. 409, 105781. doi: 10.1016/j.sedgeo.2020.105781
- Liu, E. T., Yan, D. T., Pei, J. X., Lin, X. D., and Zhang, J. F. (2023). Sedimentary architecture and evolution of a Quaternary sand-rich submarine fan in the South China Sea. *Front. Mar. Science*. 10. doi: 10.3389/fmars.2023.1280763

## Conflict of interest

Authors GF, ZY, WL, QZ, XW were employed by company PetroChina.

The remaining authors declare that the research was conducted in the absence of any commercial or financial relationships that could be construed as a potential conflict of interest.

## Publisher's note

All claims expressed in this article are solely those of the authors and do not necessarily represent those of their affiliated organizations, or those of the publisher, the editors and the reviewers. Any product that may be evaluated in this article, or claim that may be made by its manufacturer, is not guaranteed or endorsed by the publisher.

- Mayall, M., Jones, E., and Casey, M. (2006). Turbidite channel reservoirs—Key elements in facies prediction and effective development. *Mar. Petroleum Geology*, 23, 821–841. doi: 10.1016/j.marpetgeo.2006.08.001
- Mutti, E., and Ricci Lucchi, F. (1978). Turbidites of the northern apennines: Introduction to facies analysis. *Int. Geology Review*, 20, 125–166. doi: 10.1080/00206817809471524
- Normark, W. R. (1978). Fan valleys, channels, and depositional lobes on modern submarine fans: characters for recognition of sandy turbidite environments. *AAPG Bulletin*, 62, 912–931. doi: 10.1306/C1EA4F72-16C9-11D7-8645000102C1865D
- Orsolya, S., Péter, S., Imre, M., Anna, H., Gábor, B., Daniel, W., et al. (2013). Aggradation and progradation controlled clinoforms and deep-water sand delivery model in the Neogene Lake Pannon, Makó Trough, Pannonian Basin, SE Hungary. *Global Planetary Change*, 103, 149–167. doi: 10.1016/j.gloplacha.2012.05.026
- Pickering, K. T., and Hiscott, R. N. (2015). *Deep marine systems: processes, deposits, environments, tectonic and sedimentation* (Oxford: American Geophysical Union and Wiley. John Wiley & Sons).
- Piper, D. J. W., and Normark, W. R. (2001). Sandy fans—from Amazon to Hueneme and beyond. *AAPG Bulletin*, 85, 1407–1438. doi: 10.1306/8626CACD-173B-11D7-8645000102C1865D
- Portnov, A., Cook, A. E., Sawyer, D. E., Yang, C., Hillmn, J. I., and Waite, W. F. (2019). Clustered BSRs: Evidence for gas hydrate-bearing turbidite complexes in folded regions, example from the Perdido Fold Belt, northern Gulf of Mexico. *Earth Planetary Sci. Letters*, 528, 115843. doi: 10.1016/j.epsl.2019.115843
- Prélat, A., Covault, J. A., Hodgson, D. M., Fildani, A., and Flint, S. S. (2010). Intrinsic controls on the range of volumes, morphologies, and dimensions of submarine lobes. *Sedimentary Geology*, 232, 66–76. doi: 10.1016/j.sedgeo.2010.09.010
- Qiu, N., Wang, Z. W., Wang, Z. F., Sun, Z. P., Sun, Z., and Zhou, D. (2014). Tectonostratigraphic structure and crustal extension of the Qiongdongnan basin, northern South China Sea. *Chin. J. Geophysics*, 57, 3189–3207. doi: 10.6038/cjg20141008
- Reading, H. G., and Richards, M. (1994). Turbidite systems in deepwater basin margins classified by grain size and feeder system. *AAPG Bulletin*, 78, 792–822. doi: 10.1306/A25FE3BF-171B-11D7-8645000102C1865D
- Richards, M., Bowman, M., and Reading, H. (1998). Submarine-fan systems I: Characterization and stratigraphic prediction. *Mar. Petroleum Geology*, 15, 689–717. doi: 10.1016/S0264-8172(98)00036-1
- Romans, B. W., Castellort, S., Covault, J. A., Fildani, A., and Walsh, J. P. (2016). Environmental signal propagation in sedimentary systems across timescales. *Earth-Science Rev.* 153, 7–29. doi: 10.1016/j.earscirev.2015.07.012
- Shanmugam, G., and Moiola, R. J. (1988). Submarine fans: Characteristics, models, classification, and reservoir potential. *Earth-Science Rev.* 24, 383–428. doi: 10.1016/0012-8252(88)90064-5
- Shao, L., Li, A., Wu, G. X., Li, Q. Y., Liu, C. L., and Qiao, P. J. (2010). Evolution of sedimentary environment and provenance in Qiongdongnan Basin in the northern South China Sea. *Acta Petroli Sinica*, 31 (4), 548–552.
- Shi, H. S., Yang, J. H., Zhang, Y. Z., Gan, J., and Yang, J. H. (2019). Geological understanding innovation and major breakthrough to natural gas exploration in deep water in Qiongdongnan Basin. *China Petroleum Exploration*, 24, 691. doi: 10.3969/j.issn.1672-7703.2019.06.001
- Shultz, M. R., and Hubbard, S. M. (2005). Sedimentology, stratigraphic architecture, and ichnology of gravity-flow deposits partially ponded in a growth-fault-controlled slope minibasin, Tres Pasos Formation (Cretaceous), southern Chile. *J. Sedimentary Res.* 75, 440–453. doi: 10.2110/jsr.2005.034
- Soutter, E. L., Kane, I. A., Fuhrmann, A., Cumberpatch, Z. A., and Huuse, M. (2019). The stratigraphic evolution of onlap in siliciclastic deep-water systems: Autogenic modulation of allogenic signals. *J. Sedimentary Res.* 89, 890–917. doi: 10.2110/jsr.2019.49
- Spychala, Y. T., Hodgson, D. M., Flint, S., and Mountney, N. P. (2015). Constraining the sedimentology and stratigraphy of submarine intraslope lobe deposits using exhumed examples from the Karoo Basin, South Africa. *Sedimentary Geology*, 322, 67–81. doi: 10.1016/j.sedgeo.2015.03.013
- Talling, P. J., Paull, C. K., and Piper, D. J. (2013). How are subaqueous sediment density flows triggered, what is their internal structure and how does it evolve? Direct observations from monitoring of active flows. *Earth-Science Rev.* 125, 244–287. doi: 10.1016/j.earscirev.2013.07.005
- Walker, R. G. (1978). Deep-water sandstone facies and ancient submarine fans: Models for exploration for stratigraphic traps. *Am. Assoc. Petroleum Geologists Bulletin*, 62, 932–966. doi: 10.1306/C1EA4F77-16C9-11D7-8645000102C1865D
- Wang, H., Lu, Y. C., Liao, Y. T., Wang, Z. F., and Li, X. S. (2004). Sequence architecture and favorable reservoir prediction of Sanya Formation in the central and eastern Qiongdongnan Basin. *Earth Science—Journal China Univ. Geosciences*, 29, 609–614. doi: 10.3321/j.issn:1000-2383.2004.05.017
- Weimer, P., Slatt, R. M., Bouroullec, R., Fillon, R., Pettingill, H., and Pranter, M. (2007). Introduction to the petroleum geology of deepwater setting. *AAPG Stud. Geology*, 57, 171–276. doi: 10.1306/St571314
- Yao, G. S., Yuan, S. Q., Wu, S. G., and Zhong, C. (2008). Double provenance depositional model and exploration prospect in deepwater area of Qiongdongnan Basin. *Petroleum Explor. Dev.* 35, 685–691. doi: 10.1016/s1876-3804(09)60101-4
- Zen, H. L., Zhao, X. Z., Zhu, X. M., Jin, F. M., Dong, Y. L., Wang, Y. Q., et al. (2015). Seismic sedimentology characteristics of sub-clinoformal shallow-water meandering river delta: A case from the Suning area of Raoyang sag in Jizhong depression, Bohai Bay Basin, NE China. *Petroleum Explor. Dev.* 42, 621–632. doi: 10.1016/S1876-3804(15)30057-4
- Zhang, G. C., Qu, H. J., Zhang, F. L., Chen, S., Yang, H. Z., Zhao, Z., et al. (2019). Major new discoveries of oil and gas in global deepwaters and enlightenment. *Acta Petroli Sin.* 40, 1. doi: 10.7623/syxb201901001
- Zhao, M., Zhang, X. B., Ji, L. M., and Zhang, G. C. (2010). Characteristics of Tectonic Evolution in the Qiongdongnan Basin and brief discussion about its controlling on reservoirs. *Natural Gas Geoscience*, 21, 494–502.
- Zhao, Y. P., Wang, H., Yan, D. T., Jiang, P., Chen, S., Zhou, J. X., et al. (2020). Sedimentary characteristics and model of gravity flows in the eocene Liushagang Formation in Weixi'an depression, South China Sea. *J. Pet. Sci. Eng.* 190, 107082. doi: 10.1016/j.petrol.2020.107082
- Zhu, W. L., Zhang, G. C., and Gao, L. (2008). Geological characteristics and exploration objectives of hydrocarbons in the northern continental margin basin of South China Sea. *Acta Petroli Sinica*, 29, 1–9. doi: 10.3321/j.issn:0253-2697.2008.01.001